Synchronization of spontaneous bursting in a CO_2 laser

Riccardo Meucci,[1] Francesco Salvadori,[2,1] Mikhail V. Ivanchenko,[3,1] Kais Al Naimee,[4] Chansong Zhou,[5] F. Tito Arecchi,[2,1] S. Boccaletti,[6] and J. Kurths[7]

[1]*Istituto Nazionale di Ottica Applicata, Largo E. Fermi, 6 50125 Firenze, Italy*

[2]*Department of Physics, Università di Firenze, Italy*

[3]*Department of Radiophysics, University of Nizhny Novgorod, Gararin Ave. 23, Nizhny Nivgorod 603950, Russia*

[4]*Department of Physics, College of Science, University of Baghdad, Baghdad, Iraq*

[5]*Institute of Physics, University of Potsdam, 10 Am Neuen Palais, D-14415, Potsdam, Germany*

[6]*CNR-Istituto dei Sistemi Complessi, Via Madonna del Piano 10, 50019 Sesto Fiorentino (FI), Italy*

[7]*Nonlinear Dynamics, University of Potsdam, Am Neuen Palais 10, 14469 Potsdam, Germany*

(Received 14 September 2006; published 27 December 2006)

We present experimental and numerical evidence of synchronization of burst events in two different modulated CO_2 lasers. Bursts appear randomly in each laser as trains of large amplitude spikes intercalated by a small amplitude chaotic regime. Experimental data and model show the frequency locking of bursts in a suitable interval of coupling strength. We explain the mechanism of this phenomenon and demonstrate the inhibitory properties of the implemented coupling.

DOI: 10.1103/PhysRevE.74.066207 PACS number(s): 05.45.Gg, 42.65.Pc

I. INTRODUCTION

Recently, synchronization of chaotic systems has attracted much attention in the scientific community [1]. In particular, synchronization of oscillations in interacting lasers is one of the most relevant problems in experimental nonlinear dynamics.

Synchronization of chaotic lasers was first observed in Nd:YAG (Nd: yttrium aluminum garnet) [2] and CO_2 lasers with a saturable absorber inside the optical cavity [3–5]. Later, synchronization of chaotic erbium doped fiber ring [6] and microchip [7] lasers were experimentally studied. Particular attention has been devoted to synchronization phenomena in semiconductor lasers in view of their impact in telecommunication systems using chaotic carriers [8–12]. Synchronization of chaotic CO_2 lasers with an intracavity electro-optic loss modulator has been extensively investigated during these years [13].

An important topic in neurodynamics is the bursting behavior [16] where a spiking regime is alternated by a quiescent state or subthreshold activity; in this way, the bursting shows two different time scales, the fast dynamics (spikes) and the slow one responsible for the alternation. In neuron arrays the bursting synchronization is important for information coding and cognitive functions [19]. The CO_2 laser with sinusoidal modulation of the cavity losses shows a similar behavior, that is, the crisis-induced intermittency [14]. For a suitable value of the modulation amplitude the system jumps between small-amplitude chaotic oscillations and an unstable periodic orbit of large amplitude [15].

In this paper we study the synchronization of bursting in two coupled CO_2 lasers and the time scales accompanying locking of bursts, focusing on the analogies with neurodynamics. Up to now, only few theoretical studies have considered coupled nonautonomous chaotic oscillators with multiple time scales [17] or coupled chaotic oscillators with multiple attractors [18]. As stressed above, lasers exhibiting bursting regimes are good candidates for this type of investigation.

The paper is organized as follows. In Sec. II, the coupling scheme between the two lasers and the experimental results are reported. In Sec. III we introduce the model and we analyze the dynamical regimes when the coupling strength is varied. In Secs. IV and V we describe the structure of the bursts and the related synchronization. Finally, Sec. VI is devoted to the conclusions.

II. EXPERIMENTAL SETUP AND RESULTS

The experimental setup is shown in Fig. 1. It consists of two single-mode lasers with intracavity electro-optic modulators. The cavity length and output mirror transmission are, respectively, $L_1=1.43$ m and $T_1=0.10$ for the first laser and $L_2=1.35$ m and $T_2=0.090$ for the second one. The decay rates are expressed as $k_{1,2}=(cT_{1,2})/(L_{1,2})$.

Both lasers are driven by a sinusoidal signal $A\sin(2\pi ft)$ provided by two phase-locked oscillators at $f=100$ kHz. The

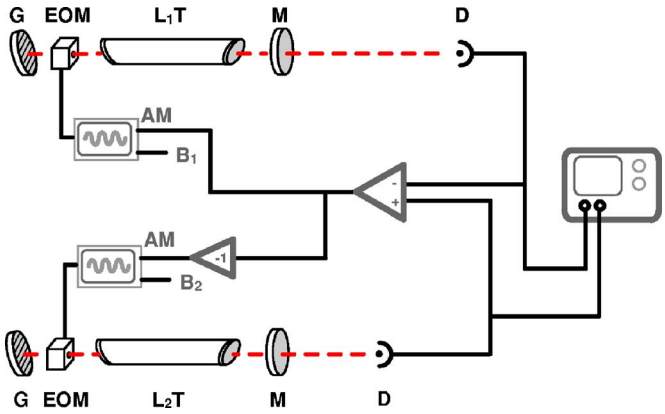

FIG. 1. (Color online) Laboratory setup consisting of two CO_2 lasers with loss modulation, partly due to an external driving and partly due to the coupling. G, grating; EOM, electro-optic modulator; L_1T and L_2T, laser tubes; M, mirror; D, detector; AM, input for amplitude modulation of the driving; $B_{1,2}$, bias voltages.

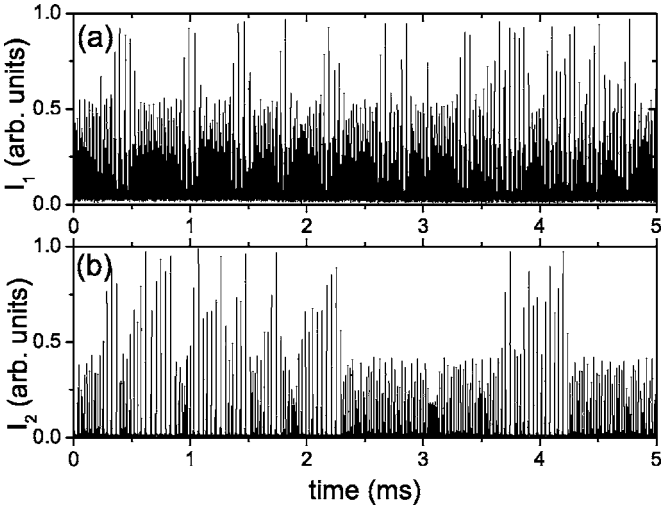

FIG. 2. Experimental time series from the first (a) and the second laser (b) in the free regime.

lasers are bidirectionally coupled through their intensities' difference used as amplitude modulation of A,

$$F_m^1 = A_1[1 + \epsilon(y_1 - x_1)]\sin(2\pi ft),$$

$$F_m^2 = A_2[1 + \epsilon(x_1 - y_1)]\sin(2\pi ft), \tag{1}$$

where x_1 (y_1) is a quantity proportional to the output intensity of the first (second) laser. The parameters of both lasers are set at values just after the onset of the interior crisis, where they display intermittent behavior as shown in Fig. 2. As the coupling strength ϵ is suitably adjusted, the jumps on the unstable orbits occur synchronously [Figs. 3(a) and 3(b)]. A more detailed analysis reveals that the two lasers are nearly phase synchronized during the small amplitude chaotic regime while during the bursts their dynamics are anticorrelated. Globally in the bursting behavior the lasers display frequency synchronization. Such a behavior is clearly shown when we report the interburst time intervals in the $x-y$ representation [Fig. 3(c)].

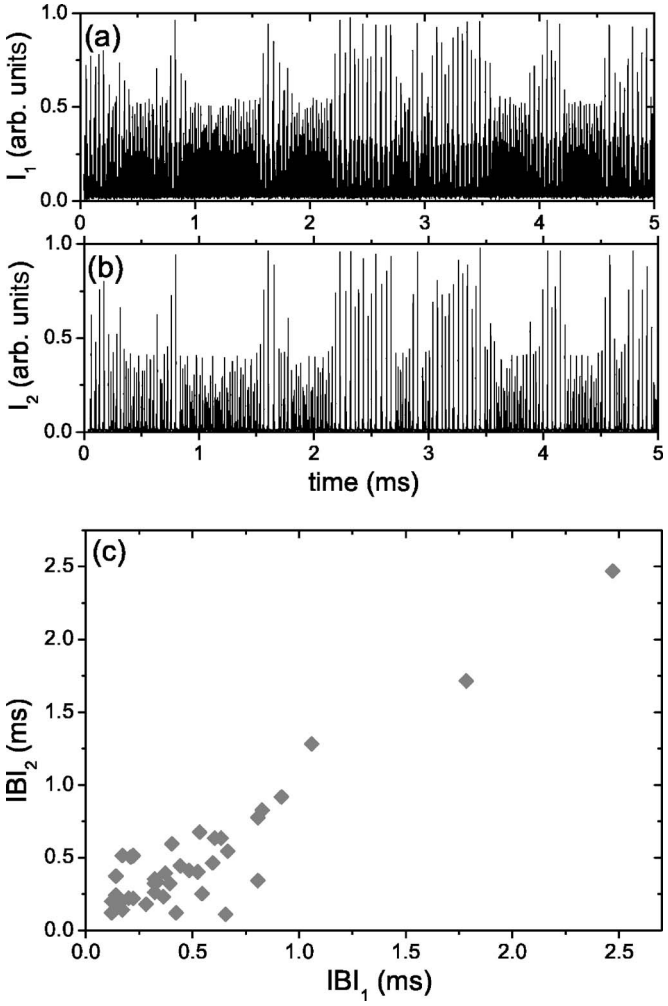

FIG. 3. Experimental time series from the first (a) and the second laser (b) in synchronized regime for ϵ=0.005; (c) plot of interbursting times of the second lasers versus the first one, showing frequency synchronization of burst events.

III. NUMERICAL MODEL AND DYNAMICAL REGIMES

The model for the two lasers is

$$\dot{x_1} = k_1 x_1\{x_2 - [1 + \alpha_1 \sin^2(F_m^1 + B_1)]\},$$

$$\dot{x_2} = -\Gamma_1 x_2 - 2k_1 x_1 x_2 + \gamma x_3 + x_4 + P_1,$$

$$\dot{x_3} = -\Gamma_1 x_3 + x_5 + \gamma x_2 + P_1,$$

$$\dot{x_4} = -\Gamma_2 x_4 + \gamma x_5 + z x_2 + z P_1,$$

$$\dot{x_5} = -\Gamma_2 x_5 + z x_3 + \gamma x_4 + z P_1, \tag{2}$$

$$\dot{y_1} = k_2 y_1\{y_2 - [1 + \alpha_2 \sin^2(F_m^2 + B_2)]\},$$

$$\dot{y_2} = -\Gamma_1 y_2 - 2k_2 y_1 y_2 + \gamma y_3 + y_4 + P_2,$$

$$\dot{y_3} = -\Gamma_1 y_3 + y_5 + \gamma y_2 + P_2,$$

$$\dot{y_4} = -\Gamma_2 y_4 + \gamma y_5 + z y_2 + z P_2,$$

$$\dot{y_5} = -\Gamma_2 y_5 + z y_3 + \gamma y_4 + z P_2, \tag{3}$$

where x_1 (y_1) represents the laser output intensity, x_2 (y_2) is the population inversion between the two resonant levels, and x_3 (y_3), x_4 (y_4), and x_5 (y_5) accounts for molecular exchanges between the two levels resonant with the radiation field and the other rotational levels of the same vibrational band; $\alpha_{1,2}=(1-2T_{1,2})/(2T_{1,2})$, $B_{1,2}$ are bias voltages, $P_{1,2}$ are pump rates, γ, Γ_1, and Γ_2 are molecular decay rates, and z is the number of sublevels in the CO_2 rotational band.

The parameter values are k_1=30, k_2=28.57, α_1=4, α_2=4.5, B_1=0.1794, B_2=0.117, Γ_1=10.0643, Γ_2=1.0643, γ=0.05, P_1=0.01987, P_2=0.0196, and z=10.

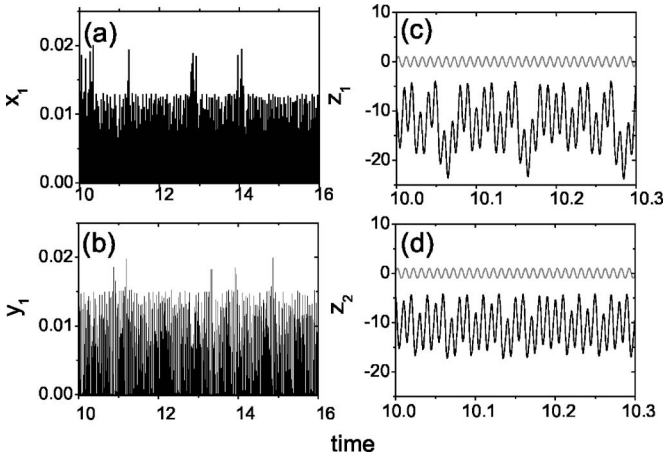

FIG. 4. Numerical time series of the two laser intensities for $\epsilon=0$: in (a),(b) are represented x_1, y_1; in (c),(d) $z_1=\ln(x_1)$, $z_2=\ln(y_1)$. The modulation signal is reported in (c),(d).

At $\epsilon=0$ the two lasers are subjected to the modulation with the same frequency $f=100$ but with different amplitudes $A_{1,2}$. The two lasers have fixed point dynamics without the forcing ($A_{1,2}=0$). They spike and burst for moderate forcing ($A_1=0.1$ and $A_2=0.129$ in the following simulations) and resume convergence to the stable fixed point at strong driving (at $A_1\approx 3.7$, $A_2\approx 2.8$).

The time series for the intensities x_1 and y_1 in the uncoupled case ($\epsilon=0$) are reported in Figs. 4(a) and 4(b) and consist of chaotic sequences of spiking events. The chaotic oscillations can be clearly seen in Figs. 4(c) and 4(d) that display the new quantities $z_1=\ln(x_1)$ and $z_2=\ln(y_1)$. Note that the spiking behavior occurs at the frequency of the modulation signal.

To study the dynamical changes due to coupling, we first calculate the largest Lyapunov exponents of the system as a function of the coupling strength. As seen in Fig. 5(a), there are many regions of ϵ, where the oscillations become periodic ($\lambda_1=0$) due to the coupling. To characterize the changes in the spiking behavior, we plot the maximal values of x_1 and y_1 as a function of ε, as shown in Fig. 5(b). It turns out that

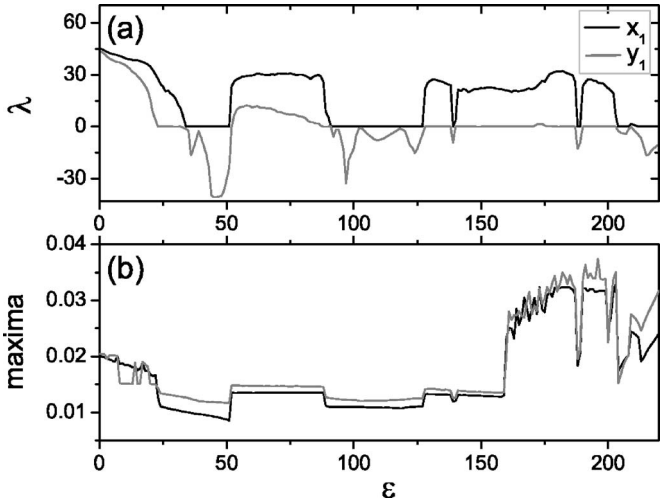

FIG. 5. (a) The largest Lyapunov exponents λ_1 and λ_2; (b) maximal intensities of x_1 (black line) and x_2 (gray line) as a function of the coupling strength ϵ.

in a large range of coupling parameter, the bursting behavior is suppressed due to coupling. An example of this latter situation is reported in Fig. 6. The maximal intensities become smaller compared to those at $\varepsilon=0$. However, we see that around $\varepsilon=160$ the lasers' maximal intensities abruptly increase. This fact is related to occasional bursting events with much larger intensities compared to usual spikes. The time series of the intensities before and after this transition are shown in Figs. 7(a) and 7(b) ($\epsilon=158$) and Figs. 7(d) and 7(e) ($\epsilon=162$). Such multiple time scale oscillations are the main subject of our study. With further increase of ε, bursting events become more frequent and at large enough coupling strength, the large amplitude spikes become ubiquitous.

IV. THE STRUCTURE OF BURSTING PATTERNS

Large spikes constituting bursts come in specific sequences. First, let us discuss the properties of the implemented coupling. Consider the modification of the modula-

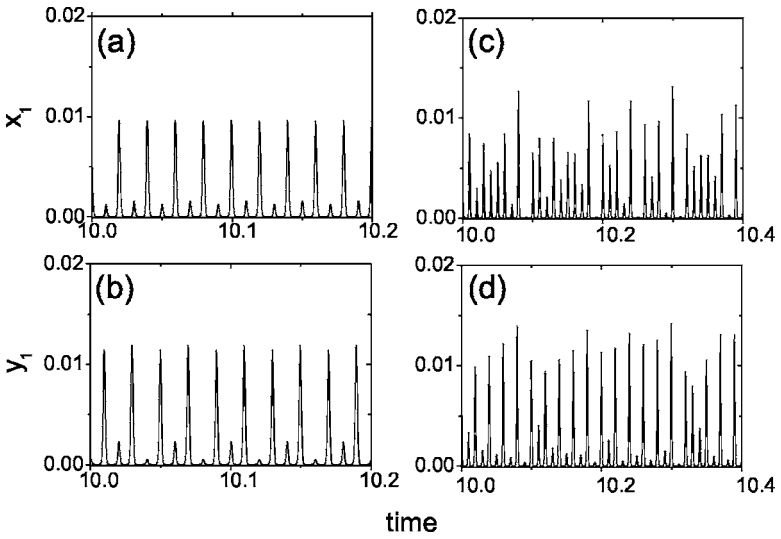

FIG. 6. Numerical time series of the two laser intensities: (a),(b) $\epsilon=40$ (periodic); (c),(d) $\epsilon=75$ (chaotic).

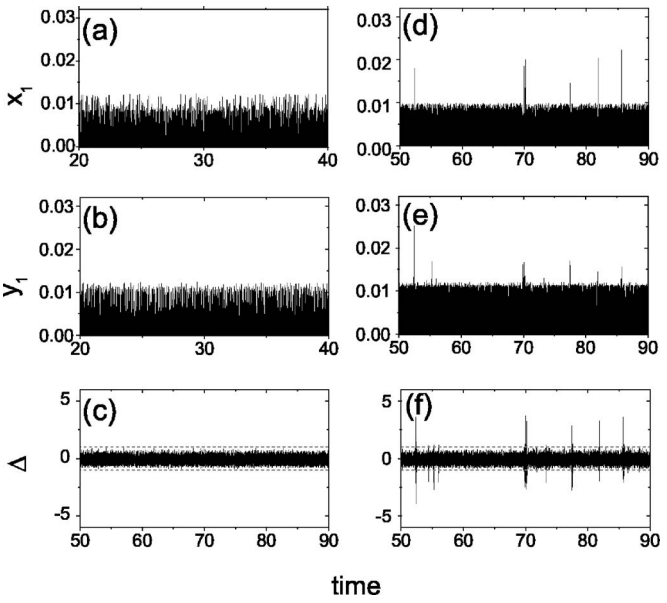

FIG. 7. Numerical time series of the two laser intensities: (a),(b),(c) $\epsilon=158$ (nonbursting); (d),(e),(f) $\epsilon=162$ (bursting).

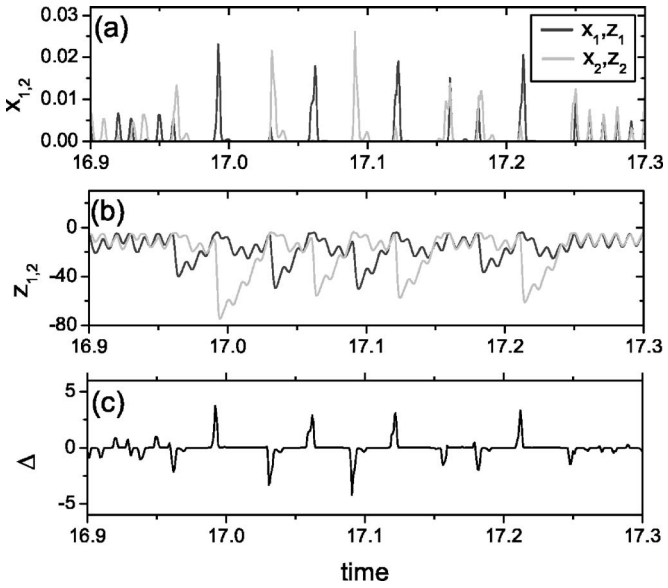

FIG. 8. Details of the bursting event around $t=17$ in Fig. 7 ($\epsilon=162$). (a) x_1, z_1 (black) and (b) y_1, z_1 (gray); (c) time series of the coupling forcing Δ in Eq. (4).

tion signals in Eqs. (1)–(3) due to the effective coupling term

$$\Delta = \epsilon(x_1 - y_1). \tag{4}$$

Note that the effective amplitude of the modulation signal is asymmetrical in the two lasers: $(1-\Delta)$ for the first laser and $(1+\Delta)$ for the second. It follows that, while a large spike in one of the lasers results in large effective coupling $|\Delta|>1$ [Figs. 7(c) and 7(f)], the effective amplitude of the modulation signal becomes large only in this counterpart. The effect is twofold. First, large effective amplitude of modulation inhibits oscillations in the laser. Second, the inhibited laser recovers more quickly than the inhibiting one, and in its turn produces a large spike. The described details of the bursting event (around $t=17$ in Fig. 7) are illustrated in Fig. 8 within a much smaller time window. The *alternating large spikes* in the two lasers during this short epoch appear as synchronized bursting events on large time scales in Fig. 7.

With increasing ϵ, the criterion $|\Delta|>1$ becomes easier to fulfill, and we observe more frequent bursting behavior. The discussed mechanism also implies that during the intervals of low-amplitude spiking the interaction between lasers is too small to provide alternation of spikes, and they occur following the modulation signal, i.e., practically at the same moments.

The same pattern is observed in experiments (Fig. 9). Small amplitude spikes are strongly correlated to the modulation signal and thus occur almost simultaneously. Large amplitude spikes alternate, with the time interval between the closest ones in two lasers being an integer of the modulation period T_f.

These findings reveal pronounced *inhibitory nature* of the implemented coupling between two lasers in the regime of burst generation. It results in the *alternating* or *antiphase* dynamics of large amplitude spikes, a typical feature of collective dynamics in inhibitory coupled neurons [16]. Such a phenomenon is different from synchronization and antisynchronization of chaotic power drop-outs and jump-ups found in coupled semiconductor lasers [9] as well as from chaos synchronization in optically coupled semiconductor lasers. In the latter case the time lag between the dynamics is imposed by the propagation of light between the two lasers [8].

V. FREQUENCY LOCKING OF BURSTS

Numerical simulations allow for extensive analysis of collective dynamics of bursting events on large time scales (up to 10^7 t.u.) and interval of the coupling strength. The bursting average frequency in each laser is given by

$$\Omega_{1,2} = \lim_{t\to\infty} n_{1,2}(t)/t, \tag{5}$$

where $n_{1,2}(t)$ is the number of bursts occurring from the initial moment up to the time t. The phase of bursting reads

$$\phi_{1,2}(t) = 2\pi\frac{t - t(n_{1,2})}{t(n_{1,2}+1) - t(n_{1,2})} + 2\pi n_{1,2},$$
$$t(n_{1,2}) \le t < t(n_{1,2}+1), \tag{6}$$

$t(n_{1,2})$ being the moment of the beginning of the $n_{1,2}$th burst in the respective laser. The criterion for the onset of a burst was that the amplitude of a spike exceeds a threshold value of 0.015, while the time separation of the previous large spike took place not larger than $80T_f$ ago (we recall that $T_f=7$ in the numerical model).

In Fig. 10(a) we plot the normalized frequency difference in interacting lasers $(\Omega_1-\Omega_2)/\Omega_1$ vs the coupling strength ε. From the reappearance of bursting at $\varepsilon\approx160$, the relative difference in their frequencies monotonously decreases and approaches zero at $\varepsilon\approx173$. Bursts in lasers remain fre-

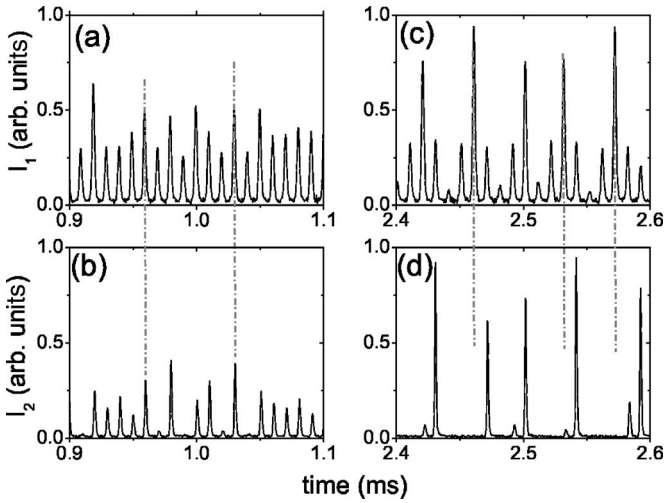

FIG. 9. Experimental time series in the low-amplitude spiking (a) and bursting regime (b).

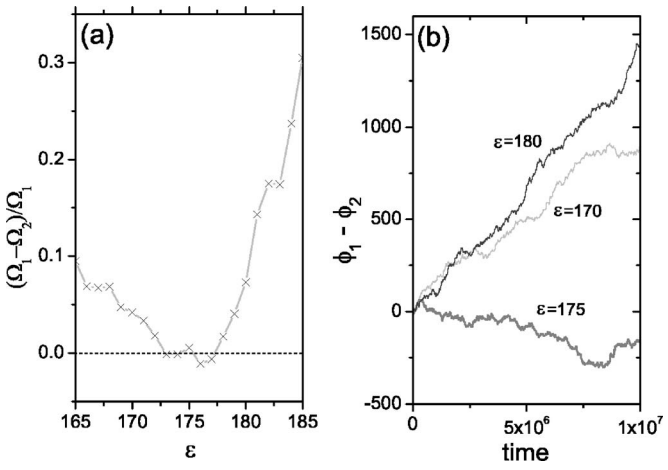

FIG. 10. Synchronization of bursts in numerical simulations: (a) the frequency locking and (b) evolution of the phase difference.

quency locked until $\varepsilon \approx 178$, when the frequency mismatch jumps to 2%. The subsequent desynchronization of the bursting is due to the qualitative change in the dynamics of interacting systems. Namely, intervals between bursts become shorter and large spikes emerge more randomly, so that bursts become indistinguishable in result. The evolution of the phase difference on large time intervals demonstrates the absence of phase locking, as the difference $\phi_1 - \phi_2$ grows unbounded even when the frequencies are locked [Fig. 10(b)]. In connection with the observed scenario of the onset of *frequency* synchronization of *bursts* and desynchronization at larger coupling, we point at the relevant synchronization-desynchronization transitions in *identical* chaotic systems [20] and nonidentical intermittent and neuronal *spiking* maps [19,21].

VI. CONCLUSIONS

In conclusion we have experimentally and numerically studied the frequency synchronization of bursting regime in two nonidentical CO_2 lasers. We have shown the antiphase synchronization inside bursting events as a consequence of an inhibitory mechanism and transitions from synchronization to desynchronization at large coupling. The desynchronization of the bursting is due to the qualitative change in the dynamics of the interacting systems.

ACKNOWLEDGMENTS

This work was partly supported by FIRB Contract No. RBAU01B49F_002. One of the authors (M.I.) acknowledges INTAS 04-83-2816.

[1] S. Boccaletti, J. Kurths, G. V. Osipov, D. L. Valladares, and C. Zhou, Phys. Rep. **366**, 1 (2002).
[2] R. Roy and K. S. Thornburg, Phys. Rev. Lett. **72**, 2009 (1994).
[3] T. Sugawara, M. Tachikawa, T. Tsukamoto, and T. Shimizu, Phys. Rev. Lett. **72**, 3502 (1994).
[4] Y. Liu and J. R. Rios Leite, Phys. Lett. A **191**, 134 (1994).
[5] Y. Liu, P. C. de Oliveira, M. B. Danailov, and J. R. Rios Leite, Phys. Rev. A **50**, 3464 (1994).
[6] G. D. VanWiggeren and R. Roy, Science **279**, 1198 (1998).
[7] A. Uchida, T. Ogawa, M. Shinozuka, and F. Kannari, Phys. Rev. E **62**, 1960 (2000).
[8] T. Heil, I. Fischer, W. Elsässer, J. Mulet, and C. R. Mirasso, Phys. Rev. Lett. **86**, 795 (2001).
[9] I. Wedekind and U. Parlitz, Phys. Rev. E **66**, 026218 (2002).
[10] E. M. Shahverdiev, S. Sivaprakasam, and K. A. Shore, Phys. Rev. E **66**, 017206 (2002).
[11] Y. C. Koumou, P. Colet, N. Gastaud, and L. Larger, Phys. Rev. E **69**, 056226 (2004).
[12] A. Argyris *et al.*, Nature (London) **437**, 343 (2005).
[13] E. Allaria, F. T. Arecchi, A. Di Garbo, and R. Meucci, Phys. Rev. Lett. **86**, 791 (2001); R. Meucci, A. Di Garbo, E. Allaria, and F. T. Arecchi, *ibid.* **88**, 144101 (2002); F. T. Arecchi, R. Meucci, E. Allaria, A. Di Garbo, and L. S. Tsimring, Phys. Rev. E **65**, 046237 (2002); S. Boccaletti, E. Allaria, R. Meucci, and F. T. Arecchi, Phys. Rev. Lett. **89**, 194101 (2002); C. S. Zhou, J. Kurths, E. Allaria, S. Boccaletti, R. Meucci, and F. T. Arecchi, Phys. Rev. E **67**, 015205(R) (2003).
[14] R. Meucci, E. Allaria, F. Salvadori, and F. T. Arecchi, Phys. Rev. Lett. **95**, 184101 (2005).
[15] E. H. Park, M. A. Zaks, and J. Kurths, Phys. Rev. E **60**, 6627 (1999).
[16] J. Rinzel, *Lecture Notes in Biomathematics* (Springer-Verlag, Berlin, 1987), Vol. 71, pp. 251–291.
[17] I. Bove, S. Boccaletti, J. Bragard, J. Kurths, and H. Mancini, Phys. Rev. E **69**, 016208 (2004).
[18] A. N. Pisarchik, R. Jaimes-Reategui, J. R. Villalobos-Salazar, J. H. Garcia-Lopez, and S. Boccaletti, Phys. Rev. Lett. **96**, 244102 (2006).
[19] H. D. Abarbanel *et al.*, Neural Comput. **8**, 1567 (1996); N. F. Rulkov, Phys. Rev. Lett. **86**, 183 (2001); M. Dhamala, V. K.

Jirsa, and M. Ding, *ibid.* **92**, 074104 (2004); I. Belykh, E. de Lange, and M. Hasler, *ibid.* **94**, 188101 (2005).

[20] L. M. Pecora and T. L. Carroll, Phys. Rev. Lett. **80**, 2109 (1998); L. M. Pecora, Phys. Rev. E **58**, 347 (1998).

[21] G. V. Osipov, M. V. Ivanchenko, J. Kurths, and B. Hu, Phys. Rev. E **71**, 056209 (2005); M. V. Ivanchenko, G. V. Osipov, V. D. Shalfeev, and J. Kurths, Phys. Rev. Lett. **93**, 134101 (2004).